PARAMETRIC STUDY ON THE SOUND ABSORPTION PROPERTIES OF 3D-PRINTED OCTET-TRUSS LATTICE STRUCTURES

MARTIN VASINA[1], ADAM BURECEK[1], LUMIR HRUZIK[1], TOMAS POLASEK[1], MARIAN LEDVON[1], DAVID KOLAR[1], RICHARD LENHARD[2], MICHAL KOZDERA[3]

[1]Department of Hydromechanics and Hydraulic Equipment, Faculty of Mechanical Engineering, VSB-Technical University of Ostrava, Czech Republic

[2]Department of Power Engineering, Faculty of Mechanical Engineering, University of Zilina, Slovakia

[3]OCHI - INZENYRING, spol. s r.o., Nakladni 3179/1, 702 00 Moravska Ostrava, Czech Republic

DOI: 10.17973/MMSJ.2025_12_2025102

e-mail to corresponding author: martin.vasina@vsb.cz

Noise is a significant environmental factor that must be eliminated by appropriate means. This study investigates the acoustic insulation properties of 3D-printed porous materials with an octet-truss lattice structure, fabricated using fused filament fabrication (FFF) technology. The sound insulation performance of the tested materials was evaluated based on the frequency dependent sound absorption coefficient, which was experimentally determined using an acoustic impedance tube. In this work, several parameters affecting the sound absorption properties of the investigated lattice material structures were systematically analysed, including volume ratio, sample thickness, excitation frequency, and the presence of air gaps. Based on the findings, specific recommendations are proposed to enhance the sound absorption characteristics of the octet-truss lattice structures and thereby reduce unwanted noise.

KEYWORDS

sound absorption, 3D printing, octet-truss lattices, excitation frequency, volume ratio

1 INTRODUCTION

At present, there is a strong emphasis on sustainability and environmental protection. Numerous factors can negatively influence environmental quality, including noise, air and water pollution, inadequate lighting conditions, and exposure to radioactive radiation [Sharma 2022, Zielinska-Dabkowska 2023, Hahad 2022, Wei 2024]. Therefore, comprehensive measures must be implemented to mitigate these impacts and contribute to the improvement of overall quality of life.

Noise can be defined as an undesirable sound that pollutes the environment. When noise is continuous and exceeds certain levels, it can have negative effects on health. An important aspect of mitigating noise is protecting the population by minimizing exposure to noise sources and reducing overall noise levels. This can be achieved through the implementation of new technical solutions and technologies, including devices designed to generate less noise [Magiera 2021].

One way to reduce noise is through passive methods using appropriate soundproofing materials [Rajappan 2017]. These materials typically have a porous, fibrous, or spongy structure, including polyurethane foam, mineral wool, glass fiber, perforated panels, and eco-friendly natural materials [Kalauni 2019]. They dissipate acoustic energy primarily through heat loss caused by the friction of air molecules against the pore walls and the viscous losses of airflow within the material's structure [Feng 2025].

3D printing appears to be a promising technology for the production of sound-absorbing materials, as it enables the creation of complex three-dimensional structures that would be difficult or impossible to manufacture using conventional methods [Sekar 2024, Subeshan 2025]. The main advantages over traditional manufacturing include rapid prototyping, design flexibility, reduced material waste, and the ability to combine different types of materials into a single structure to achieve higher sound absorption efficiency [Islam 2024]. In this way, 3D printing technology can be used to produce customized acoustic materials for various applications, including sound insulation in buildings, vehicles, and industry [Setaki 2023, Qin 2024, Li 2024].

The aim of this paper is to investigate the sound absorption properties of 3D-printed recycled PETG samples with an octet-truss lattice structure, fabricated using fused filament fabrication (FFF) technology. Several factors influencing the sound damping ability of the porous samples were examined, including sample thickness, material volume ratio, the size of the air gap behind the sample inside the acoustic impedance tube, and the excitation frequency of acoustic waves.

2 SOUND ABSORPTION PROPERTIES OF MATERIALS

When acoustic energy propagates from a sound source toward an obstacle, part of the incident energy is reflected by the obstacle, while the remainder is absorbed [Koizumi 2002]. Based on this energy balance, the material's ability to absorb sound is quantified by the sound absorption coefficient α, as defined by the following equation:

$$\alpha = \frac{E_A}{E_I} = 1 - \frac{E_R}{E_I} \quad (1)$$

Where:
E_A – absorbed acoustic energy (J),
E_I – incident acoustic energy (J),
E_R – reflected acoustic energy (J).

In general, materials exhibit better sound absorption performance at higher values of the sound absorption coefficient (i.e., $\alpha \rightarrow 1$). Conversely, when $\alpha = 0$, all incident acoustic energy is reflected by the obstacle. The value of the sound absorption coefficient is influenced by various factors, including the type of material, manufacturing method, acoustic wave frequency, material thickness, density and internal structure, surface geometry, and others [Tiuc 2014, Mohammadi 2025].

The effect of acoustic wave frequency is taken into account in the Noise Reduction Coefficient (*NRC*), which is defined as the arithmetic average of the sound absorption coefficients measured at frequencies of 250, 500, 1000, and 2000 Hz [Sung 2016]. In addition, the mean sound absorption coefficient α_m [–] was determined as the arithmetic mean of the sound absorption coefficient values measured in the frequency range from 150 to 6600 Hz, using a frequency step of 1 Hz.

3 MATERIALS

3.1 Materials

The samples used in this study were produced from recycled polyethylene terephthalate glycol (PETG) supplied by Nobufil GmbH, Krems an der Donau, Austria. The raw material was a white filament with a diameter of 1.75 mm, made from recycled industrial waste sourced from European suppliers. The selection of recycled PETG is in accordance with current trends in the circular economy and sustainable production. PETG was chosen as a suitable material for additive manufacturing of functional samples due to its toughness, dimensional stability, and relatively low processing temperature.

3.2 Samples production

3D-printed open-porous samples examined in this study were produced using FFF technology. A key advantage of this method is its ability to create components with complex geometries, including internal cavities and cellular structures, which are difficult or impossible to achieve using conventional methods such as machining, injection molding, or casting without additional support manufacturing. Such designs are increasingly used in applications where a combination of low weight and specific functional properties is required, including enhanced acoustic absorption. In these applications, the geometry of the pores, their distribution, and their connectivity are critical factors that determine their performance.

The virtual models of the studied samples were created using SolidWorks 2016 software. An octet-truss structure was selected as the basic cellular motif (see Figure 1), consisting of a periodically repeating arrangement of octahedral and tetrahedral units. Each node of this bar grid is connected by twelve bars, providing high isotropic stiffness. This type of lattice is known for its advantageous combination of mechanical stability and low density. However, in this study, it was primarily investigated for its acoustic performance.

The samples were fabricated using a Bambu Lab X1C Carbon desktop 3D printer (from Shenzhen Tuozhu Technology Co., Ltd., Shenzhen, China) equipped with a 0.4 mm nozzle. The slicer settings were chosen as a compromise between print resolution, manufacturing time, and structural stability of the resulting samples. The layer height was set to 0.16 mm and the extrusion width to 0.42 mm, providing sufficient resolution for printing thin rods while maintaining a reasonable production speed. The material infill was defined as a grid with a nominal density of 15%. However, due to the rod diameter (*d*), the internal infill was practically absent, and the structure was primarily formed by the octet-truss geometry itself. The outer walls were printed with two perimeters, the top layers with five, and the bottom layers with three, ensuring adequate closure of the external surfaces of the samples.

The individual sample variants differed in their geometric parameters, including element side length *l*, and rod diameter *d*, resulting in different porosities, as summarized in Table 1. All samples used for the evaluation of sound absorption properties were manufactured in the shape of a cylinder with a diameter of *D* = 30 mm (see Figure 2). They were also produced with varying thicknesses (heights) *t* (i.e., 10, 30, and 50 mm) and volume ratios *VR* (i.e., 10%, 17%, 34%, and 53%), as defined by the following formula:

$$VR = \frac{V_S}{V_T} \cdot 100 \qquad (2)$$

Where:

V_S – volume of material used to manufacture the structure (m^3),

V_T – volume of the whole solid body (m^3).

A photo of 3D-printed test samples with various volume ratios *VR* is shown in Figure 3.

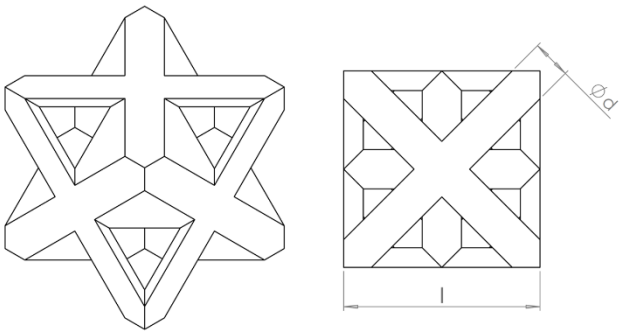

Figure 1. Applied 3D-printed octet-truss structure with corresponding dimensions.

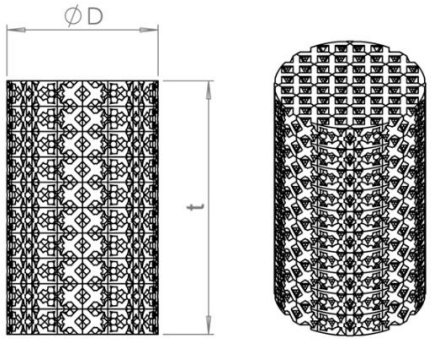

Figure 2. Visualization of a 3D-printed sample with basic dimensions.

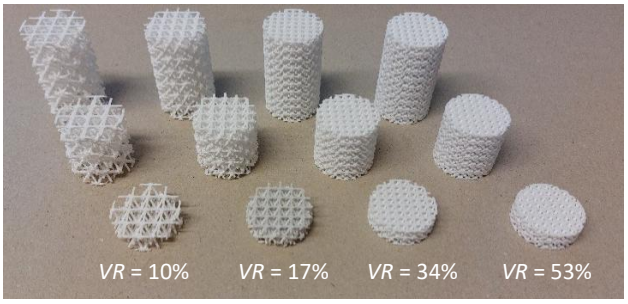

Figure 3. Photo of 3D-printed tested samples with various volume ratios *VR*.

VR [%]	*l* [mm]	*d* [mm]
10	10.0	1.0
17	7.5	1.0
34	5.0	1.0
53	5.0	1.3

Table 1. Basic parameters of 3D-printed PETG samples.

4 MEASUREMENT METHODOLOGY

Frequency dependencies of the sound absorption coefficient of the studied 3D-printed octet-truss lattices were measured by means of a three-microphone acoustic impedance tube (AED AcoustiTube) in combination with a data acquisition device (Sinus "Apollo lite") and a signal amplifier (Atlas Sound PA 604) in the frequency range of (150 – 6600) Hz (Gesellschaft für Akustikforschung Dresden mbH, Dresden, Germany). The measured results are presented using 1/3 octave band filtering. All experiments were performed at an ambient temperature of 22 °C.

Experimental measurements of the normal incidence sound absorption coefficient were performed by the transfer function method [ISO 10534-2 1998, Tubelis 2024] based on the partial standing wave principle. The transfer functions between different microphone positions are determined according to equations (3) – (5):

$$H_{12} = \frac{p_2}{p_1} \quad (3)$$

$$H_{13} = \frac{p_3}{p_1} \quad (4)$$

$$H_{23} = \frac{p_3}{p_2} \quad (5)$$

Where:
H_{12} – transfer function between microphone positions 1 and 2 (–),
H_{13} – transfer function between microphone positions 1 and 3 (–),
H_{23} – transfer function between microphone positions 2 and 3 (–),
p_1 – pressure measured by the microphone M_1 placed furthest to the sample surface (Pa),
p_2 – pressure measured by the microphone M_2 (Pa),
p_3 – pressure measured by the microphone M_3 placed closest to the sample surface (Pa).
The transfer functions for incident wave H_I (–) and transfer function for reflected wave H_R (–) are determined in the appropriate frequency band according to equations (6) and (7):

$$H_{I(160-1000\ Hz)} = \frac{p_{3I}}{p_{1I}} = e^{-jk_0\cdot(x_{12}+x_{23})} \quad (6a)$$

$$H_{I(1000-5000\ Hz)} = \frac{p_{3I}}{p_{2I}} = e^{-jk_0\cdot(x_{23})} \quad (6b)$$

$$H_{R(160-1000\ Hz)} = \frac{p_{3R}}{p_{1R}} = e^{jk_0\cdot(x_{12}+x_{23})} \quad (7a)$$

$$H_{R(1000-5000\ Hz)} = \frac{p_{3R}}{p_{2R}} = e^{jk_0\cdot(x_{23})} \quad (7b)$$

Where:
j – imaginary unit,
k_0 – wave number (m^{-1}),
x_{12} – distance between microphones 1 and 2 (m),
x_{23} – distance between microphones 2 and 3 (m).
The reflection coefficient R (–) in the appropriate frequency band is expressed by the equations:

$$R_{(160-1000\ Hz)} = \frac{H_{13}-H_{I(160-1000\ Hz)}}{H_{R(160-1000\ Hz)}-H_{12}} \cdot e^{2jk_0\cdot(x_{12}+x_{23}+x_{3s})} \quad (8a)$$

$$R_{(1000-5000\ Hz)} = \frac{H_{23}-H_{I(1000-5000\ Hz)}}{H_{R(1000-5000\ Hz)}-H_{13}} \cdot e^{2jk_0\cdot(x_{23}+x_{3s})} \quad (8b)$$

Where:
x_{3s} – distance between microphone 3 and tested sample (m).
Finally, the sound absorption coefficient α (–) is calculated using the following formula:

$$\alpha = 1 - |R|^2 \quad (9)$$

5 RESULTS AND DISCUSSION

This chapter discusses various factors affecting the sound absorption properties of the investigated 3D-printed samples, including the volume ratio, the sample thickness, the air gap size behind the sample in the impedance tube, and the excitation frequency.

5.1 *Effect of volume ratio*

The volume ratio (*VR*), defined by Equation (2), is related to the volume porosity (or density) of the investigated 3D-printed porous samples fabricated with the octet-truss lattice structure. The volume ratio effect on the sound absorption performance is shown in Figures 3 and 4. Figure 3 shows the experimentally obtained frequency dependencies of the sound absorption coefficient (α) for samples with a thickness of 10 mm and an air gap of 40 mm behind them in the impedance tube. Similarly, Figure 4 presents the influence of the volume ratio on the sound absorption performance of the tested samples with a thickness of 50 mm and no air gap behind them inside the impedance tube, as a function of their volume ratio. It is evident from these comparisons that sound absorption properties are generally increasing with increasing the sample´s volume ratio, which is proportional to the sample´s airflow resistivity. In general, increasing airflow resistivity enhances the sound absorption properties of porous materials across the entire frequency range health [Doutres 2011], but only up to an intermediate value. If the airflow resistivity becomes too high, the material becomes overly acoustically resistive, which significantly reduces its ability to absorb sound as the acoustic wave propagates through its porous structure.

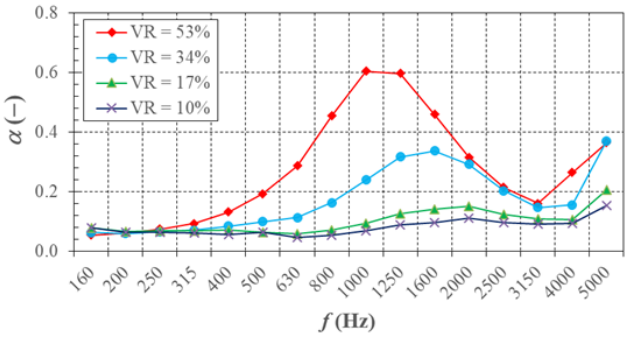

Figure 3. Effect of the volume ratio on the frequency dependencies of the sound absorption coefficient for 3D-printed PETG samples with an octet-truss lattice structure: t = 10 mm, a = 40 mm.

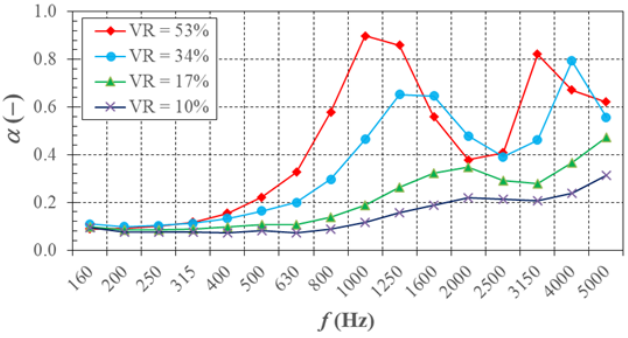

Figure 4. Effect of the volume ratio on the frequency dependencies of the sound absorption coefficient for 3D-printed PETG samples with an octet-truss lattice structure: t = 50 mm, a = 0 mm.

5.2 *Effect of sample thickness*

The sample thickness (t) is an important factor influencing the sound absorption performance of porous material structures, including the investigated 3D-printed octet-lattice structures. Figures 5 and 6 show examples of the influence of the sample thickness on sound absorption at specific volume ratios and air gap sizes. These comparisons clearly demonstrate that greater sample thickness generally increases the conversion of acoustic energy into heat during wave propagation through a 3D-printed sample, thereby enhancing the sound absorption ability of thicker materials. The positive effect of the sample thickness on sound absorption is further supported by higher values of both the noise reduction coefficient (*NRC*) and the mean sound absorption coefficient (α_m), as shown in Tables 2 and 3. This method of enhancing sound absorption is limited by increased

material consumption, which leads to higher production costs and longer manufacturing times for 3D-printed structures. One possibility for reducing material consumption is the use of sound insulation materials in combination with an air gap [Wang 2015], as described in the following chapter.

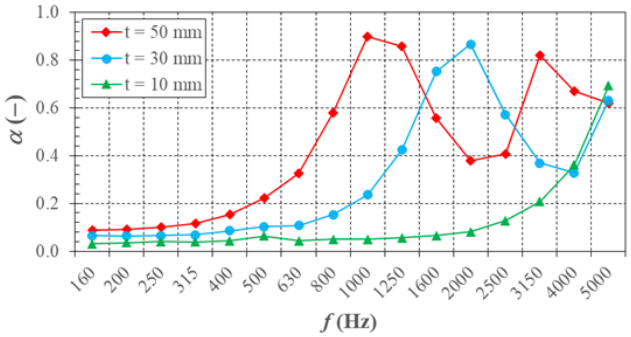

Figure 5. Effect of the sample thickness on the frequency dependencies of the sound absorption coefficient for 3D-printed PETG samples with an octet-truss lattice structure: *VR* = 53%, *a* = 0 mm.

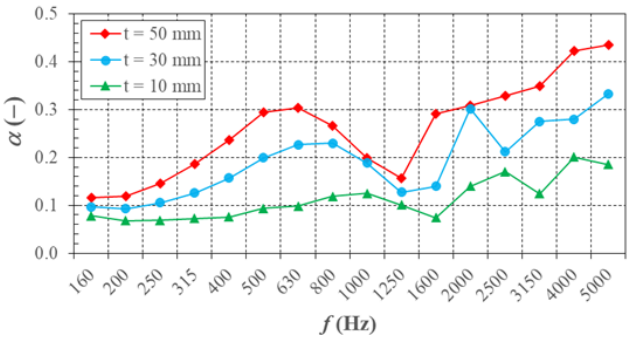

Figure 6. Effect of the sample thickness on the frequency dependencies of the sound absorption coefficient for 3D-printed PETG samples with an octet-truss lattice structure: *VR* = 17%, *a* = 100 mm.

5.3 *Effect of air gap size*

The use of an air gap behind porous materials is an effective method to enhance the sound absorption properties of the investigated 3D-printed porous structures. The effect of the air gap size on the sound absorption coefficient of the tested 3D-printed PETG samples with an octet-truss lattice structure is demonstrated in Figures 7 and 8. An increase in air gap size generally resulted in enhanced sound absorption, especially at low excitation frequencies. This phenomenon is attributed to the wavelength of sound λ, which is defined as:

$$\lambda = \frac{c}{f} \tag{10}$$

Where:
c – speed of sound in air (m·s^{-1}),
f – frequency of the incident acoustic wave (Hz).

When the investigated porous material is placed at a quarter-wavelength (i.e., $\lambda/4$) distance from a solid wall, maximum sound absorption can be achieved because the air particle velocity reaches its peak at this location (see Figure 7). Conversely, at a half-wavelength (i.e., $\lambda/2$) distance, the air particle velocity is at a minimum, resulting in a lower sound absorption coefficient [Mvubu 2019]. For these reasons, sound absorption maxima occur at odd multiples of quarter wavelengths, corresponding to the antinodes of standing waves at specific excitation frequencies:

$$f = \frac{c\cdot(2n+1)}{4\cdot(a+t/2)} \tag{11}$$

Where:
n – integer (n = 0, 1, 2…),
a – air gap size behind the tested sample in the impedance tube (m).
Similarly, sound absorption minima are obtained at even multiples of quarter wavelengths in standing-wave nodes at specific excitation frequencies:

$$f = \frac{c\cdot n}{2\cdot(a+t/2)} \tag{12}$$

The advantage of porous materials combined with an air gap is that the gap can be tuned for a given material thickness to maximize sound absorption at frequencies corresponding to odd multiples of a quarter wavelength.

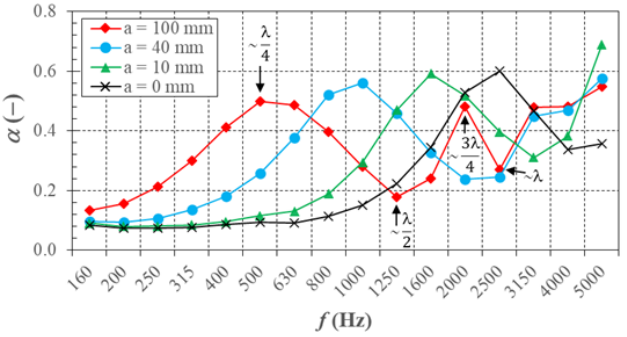

Figure 7. Effect of the air gap size on the frequency dependencies of the sound absorption coefficient for 3D-printed PETG samples with an octet-truss lattice structure: *VR* = 34%, *t* = 30 mm.

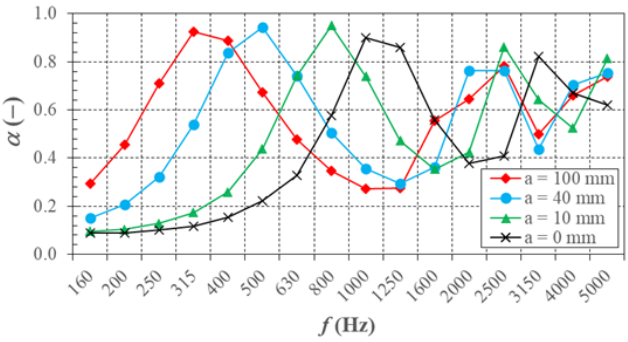

Figure 8. Effect of the air gap size on the frequency dependencies of the sound absorption coefficient for 3D-printed PETG samples with an octet-truss lattice structure: *VR* = 53%, *t* = 50 mm.

5.4 *Effect of excitation frequency*

As shown above in Figures 3-8, sound absorption properties of the studied 3D-printed PETG samples fabricated with an octet-truss lattice structure are strongly influenced by the excitation frequency (*f*) of acoustic waves. It is obvious that a relatively low sound absorption ability was found at low excitation frequencies. This phenomenon was confirmed by the *NRC* coefficient (i.e., the arithmetic average of sound absorption coefficients at frequencies of 250, 500, 1000, and 2000 Hz), which reflects the sound absorption properties of materials at low excitation frequencies, as shown in Table 2. It is evident that the *NRC* coefficient generally increased with increasing sample thickness, volume ratio, and air gap size behind the measured specimen inside the acoustic impedance tube. The highest *NRC* value (i.e., 0.597) was observed for the sample with a thickness of 50 mm, a volume ratio of 53%, and an air gap of 40 mm.

A similar trend, namely an increase in the sound absorption properties of the investigated 3D-printed PETG samples with increasing sample thickness, volume ratio, and air gap size, was also observed for the mean sound absorption coefficient α_m calculated over the entire frequency range of 150–6600 Hz, as

given in Table 3. This phenomenon is particularly characteristic of smaller sample thicknesses and volume ratios. Conversely, at the maximum sample thickness (i.e., 50 mm) and higher volume ratios (i.e., 34 and 53%), the average sound absorption properties of the tested samples were found to be very similar and practically independent of the air gap size. The best average sound absorption properties (i.e., $\alpha_m \cong 0.62$) were obtained for the samples with a thickness of 50 mm and a volume ratio of 53%, regardless of the air gap size behind them.

It can be concluded that the highest values of the calculated *NRC* and α_m coefficients, highlighted in blue in Tables 2 and 3, were generally obtained for samples manufactured with the highest volume ratio and thickness.

From the measured frequency dependencies, it was also found that the maximum sound absorption coefficient α_{max} was very close to 1 for the sample with a thickness of 30 mm, a volume ratio of 53%, and an air gap of 40 mm at an excitation frequency of 4869 Hz.

VR [%]	*t* [mm]	*a* [mm]			
		0	10	40	100
10	10	0.035	0.062	0.078	0.081
	30	0.085	0.095	0.115	0.143
	50	0.126	0.133	0.147	0.168
17	10	0.054	0.058	0.087	0.108
	30	0.099	0.123	0.163	0.209
	50	0.169	0.189	0.217	0.237
34	10	0.056	0.095	0.171	0.177
	30	0.232	0.248	0.295	0.370
	50	0.303	0.344	0.391	0.398
53	10	0.052	0.210	0.294	0.439
	30	0.331	0.335	0.395	0.462
	50	0.397	0.424	**0.597**	0.565

Table 2. Measured values of the noise reduction coefficient *NRC* [–] of the studied 3D-printed PETG samples.

VR [%]	*t* [mm]	*a* [mm]			
		0	10	40	100
10	10	0.074	0.104	0.112	0.132
	30	0.156	0.175	0.181	0.201
	50	0.228	0.240	0.245	0.264
17	10	0.096	0.140	0.143	0.157
	30	0.221	0.259	0.260	0.272
	50	0.330	0.349	0.353	0.364
34	10	0.184	0.249	0.236	0.248
	30	0.392	0.450	0.435	0.434
	50	0.537	0.579	0.570	0.568
53	10	0.352	0.327	0.310	0.310
	30	0.535	0.520	0.511	0.512
	50	**0.629**	0.621	0.620	0.627

Table 3. Measured values of the mean sound absorption coefficient α_m [–] of the studied 3D-printed PETG samples.

6 CONCLUSIONS

The aim of this paper was to investigate the factors influencing the sound absorption properties of 3D-printed recycled PETG materials with an octet-truss lattice structure, fabricated using fused filament fabrication technology. The parameters considered were volume ratio, sample thickness, air gap size, and the excitation frequency of incident acoustic waves. The results demonstrated that all these factors had a significant influence on the sound absorption performance of the investigated porous samples. In general, higher sound absorption was achieved with increasing sample thickness, volume ratio, and air gap size behind the samples in the impedance tube. With respect to excitation frequency, low sound absorption was typically observed at lower excitation frequencies. However, at certain frequencies, depending on the specific sample, nearly ideal sound absorption ($\alpha_{max} \approx 1$) was recorded, with almost complete suppression of sound reflection from the surface of the 3D-printed material. This indicates that nearly all incident acoustic energy was absorbed by the lattice material structure. Nevertheless, the frequency bands exhibiting such high absorption were relatively narrow for the given sample.

3D printing is a developing and promising technology that finds applications in many areas of our lives. It enables the production of lightweight materials with various shapes and structures that cannot be manufactured using conventional technologies such as injection molding, casting, or machining. Therefore, the use of 3D printing contributes to savings in time, materials, and energy. For these reasons, it is also possible to design new types of 3D-printed porous structures that exhibit high sound absorption across a wide frequency range, which may be the subject of future research. In this way, 3D printing can significantly contribute to enhancing both the sustainability and the quality of our environment.

ACKNOWLEDGMENTS

This paper was created as part of the project No. CZ.02.01.01/00/22_008/0004631 “Materials and technologies for sustainable development” within the Jan Amos Komensky Operational Program financed by the European Union and from the state budget of the Czech Republic. The work presented in this paper was supported by a grant SGS „Non-stationary flow in fluid systems and its damping." SP2025/017.

DATA AVAILABILITY STATEMENT

The data that support the findings of this study are openly available in [Zenodo] at https://doi.org/10.5281/zenodo.17205964 [Vašina 2025].

REFERENCES

[Sharma 2022] Sharma, H. Environmental Pollution: A Great Hazard in The Survival of Man. Central Asian Journal of Medical and Natural Sciences, October 2022, Vol.3, No.5, pp 184-193. ISSN 2660-4159

[Zielinska-Dabkowska 2023] Zielinska-Dabkowska, K. M., et al. Reducing nighttime light exposure in the urban environment to benefit human health and society. Science, June 2023, Vol.380, No.6650, pp 1130-1135. ISSN 0036-8075

[Hahad 2022] Hahad, O., et al. Cerebral consequences of environmental noise exposure. Environment International, July 2022, Vol.165, 107306. ISSN 0160-4120

[Wei 2024] Wei, Y., et al. Fukushima's Radioactive Water Threatens Coastal Groundwater. Environmental Science & Technology, October 2024, Vol.58, No.42, pp 18450-18455. ISSN 0013-936X

[Magiera 2021] Magiera, A. and Solecka, J. Environmental noise, its types and effects on health. Roczniki Państwowego Zakładu Higieny, March 2021, Vol.72, No.1, pp 41-48. ISSN 0035-7715

[Rajappan 2017] Rajappan, S., et al. An Insight into the Composite Materials for Passive Sound Absorption. Journal of Applied Sciences, June 2017, Vol.17, No.7, pp 339-356. ISSN 1812-5654

[Kalauni 2019] Kalauni, K. and Pawar, S. J. A review on the taxonomy, factors associated with sound absorption and theoretical modeling of porous sound absorbing materials. Journal of Porous Materials, December 2019, Vol.26, No.6, pp 1795-1819. ISSN 1380-2224

[Feng 2025] Feng, Z. T. and Liu, Y. J. The latest research status of porous sound-absorbing materials. Journal of Polymer Engineering, March 2025, Vol.45, No.3, pp 207-225. ISSN 0334-6447

[Sekar 2024] Sekar, V., et al. Additively manufactured metamaterials for acoustic absorption: a review. Virtual and Physical Prototyping, December 2024, Vol.19, No.1, e2435562. ISSN 1745-2759

[Subeshan 2025] Subeshan, B., et al. Fabricating Three-Dimensional Metamaterials Using Additive Manufacturing: An Overview. Journal of Manufacturing and Materials Processing, October 2025, Vol.9, No.10, 343. ISSN 2504-4494

[Islam 2024] Islam, M. A., et al. Additive manufacturing in polymer research: Advances, synthesis, and applications. Polymer Testing, March 2024, Vol.132, 108364. ISSN 0142-9418

[Setaki 2023] Setaki, F., et al. 3D-printed sound absorbers: compact and customisable at broadband frequencies. Architecture, Structures and Construction, February 2023, Vol.3, pp 203-215. ISSN 2730-9886

[Qin 2024] Qin, X. C., et al. Research on the design and noise reduction performance of periodic noise barriers based on nested structure. Journal of Cleaner Production, October 2024, Vol.476, 143708. ISSN 0959-6526

[Li 2024] Li, X., et al. 3D-Printed Lattice Structures for Sound Absorption: Current Progress, Mechanisms and Models, Structural-Property Relationships, and Future Outlook. Advanced Science, January 2024, Vol.11, No.4, 2305232. ISSN 2198-3844

[Koizumi 2002] Koizumi, T., et al. The development of sound absorbing materials using natural bamboo fibers. High Performance Structures and Materials, March 2002, Vol.4, pp 157–166. ISSN 1469-0071

[Tiuc 2014] Tiuc, A. E., et al. The Analysis of Factors That Influence the Sound Absorption Coefficient of Porous Materials. Romanian Journal of Acoustics and Vibration, January 2014, Vol.11, No.2, pp 105–108. ISSN 1584-7284

[Mohammadi 2025] Mohammadi, M., et al. A Comprehensive Review of Factors Influencing the Sound Absorption Properties of Micro-Perforated Panel Structures. Journal of Vibration Engineering & Technologies, June 2025, Vol.13, No.5, 319. ISSN 2523-3920

[Sung 2016] Sung, G., et al. Fabrication of polyurethane composite foams with magnesium hydroxide filler for improved sound absorption. Journal of Industrial and Engineering Chemistry, December 2016, pp 99–104. ISSN 1226-086X

[ISO10534-2 1998] Standard ISO 10534-2:1998. Acoustics-Determination of Sound Absorption Coefficient and Impedance in Impedance Tubes-Part 2: Transfer-Function Method.

[Tubelis 2024] Tubelis, J., et al. Acoustic Properties of Recycled Polyurethane Foam Waste and Polyvinyl Acetate Composites. Environmental and Climate Technologies, January 2024, Vol.28, No.1, pp 749–759. ISSN 1691-5208

[Doutres 2011] Doutres, O., et al. Effect of the microstructure closed pore content on the acoustic behavior of polyurethane foams. Journal of Applied Physics, September 2011, Vol.110, No.6, 064901. ISSN 0021-8979

[Wang 2015] Wang, X. P., et al. Research on the sound absorption characteristics of porous metal materials at high sound pressure levels. Advances in Mechanical Engineering, May 2015, Vol.7, No.5, 1687814015575429. ISSN 1687-8132

[Mvubu 2019] Mvubu, M. B., et al. Effects of air gap, fibre type and blend ratio on sound absorption performance of needle-punched non-woven fabrics. Journal of Engineered Fibers and Fabrics, April 2019, Vol.14. ISSN 1558-9250

[Vasina 2025] Vasina, M., et al. Parametric study on the sound absorption properties of 3D-printed octet-truss lattice structures. Zenodo. https://doi.org/10.5281/zenodo.17205964.

CONTACTS:

Assoc. Prof. Ing. Martin Vasina, Ph.D.
VSB - Technical University of Ostrava, Department of Hydromechanics and Hydraulic Equipment,
17. listopadu 2172/15, CZ-708 00 Ostrava-Poruba
+420 597 995 210, martin.vasina@vsb.cz